Circularly permuted variants of the green fluorescent protein

Simon Topell, Jens Hennecke[1], Rudi Glockshuber*

Institut für Molekularbiologie und Biophysik, Eidgenössische Technische Hochschule-Hönggerberg, CH-8093 Zürich, Switzerland

Received 30 July 1999

Abstract **Folding of the green fluorescent protein (GFP) from *Aequorea victoria* is characterized by autocatalytic formation of its p-hydroxybenzylideneimidazolidone chromophore, which is located in the center of an 11-stranded β-barrel. We have analyzed the in vivo folding of 20 circularly permuted variants of GFP and find a relatively low tolerance towards disruption of the polypeptide chain by introduction of new termini. All permuted variants with termini in strands of the β-barrel and about half of the variants with termini in loops lost the ability to form the chromophore. The thermal stability of the permuted GFPs with intact chromophore is very similar to that of the wild-type, indicating that chromophore-side chain interactions strongly contribute to the extraordinary stability of GFP.**

Key words: Circular permutation;
Green fluorescent protein (GFP); Protein folding; Stability

1. Introduction

The close proximity of N- and C-termini observed in many 3-dimensional protein structures [1] has been used in the past to perform circular permutation experiments on many different proteins. Since the first synthesis of a circularly permuted protein by chemical ligation of the termini in bovine pancreatic trypsin inhibitor (BPTI) and enzymatic cleavage of the circular protein by trypsin [2], molecular cloning techniques have been used for rational construction of circularly permuted protein variants through connecting the natural termini with linker peptides of appropriate length and introduction of new termini into surface-exposed loop regions ([3,4] and references cited therein). These studies have led to the conclusion that designed circularly permuted proteins with new termini in loops generally fold to a functional 3-dimensional structure and that the position of the termini is not critical for folding. In 1996 a new experimental approach has been introduced by Graf and Schachman [5] by which the catalytic subunit of aspartate transcarbamoylase was subjected to random circular permutation, and active permuted variants were identified by selection techniques. This study revealed that even the introduction of the new termini into regular secondary structures may be tolerated and allows folding to a biologically active conformation [5]. Using the periplasmic disulfide oxidoreductase DsbA, a monomeric two-domain protein of 189 residues as a model, we have recently performed a systematic random circular permutation study in which every regular secondary structure and every loop region of DsbA was disrupted by introduction of new termini [4]. This experiment confirmed that circularly permuted proteins can still fold after introduction of the new termini into regular secondary structures and also identified segments of the polypeptide chain that are essential for folding [4].

Here we extend our circular permutation studies on the green fluorescent protein (GFP) from *Aequorea victoria* as a new model system for circular permutations in a one-domain protein. GFP is a monomeric 238-residue protein with a unique structural motif consisting of an 11-stranded β-barrel [6–8]. The barrel harbors a coaxial helical segment that contains the GFP fluorophore, a p-hydroxybenzylideneimidazolidone moiety which is formed by autocatalytic intramolecular cyclization of the tripeptide segment Ser^{65}-Tyr^{66}-Gly^{67} and subsequent air oxidation [9–14]. As GFP is extraordinarily stable against denaturation and proteolytic degradation [15,16] and can be functionally expressed both as isolated protein or fusion protein in practically any cell type, it has become the most important reporter molecule for the observation of specific processes in the living cell, e.g. the intracellular distribution of target proteins, protein/protein interactions and changes in ion concentrations and pH [17–20]. Both termini of GFP are located on top of the β-barrel and in close proximity. This, together with the possibility to identify fluorescent bacterial clones expressing functional GFP directly at the level of single colonies, makes GFP an ideal model system for circular permutation studies. In the present study, we have used a variant of GFP, termed GFPuv, that differs from the wild-type by three amino acid replacements (F99S, M153T and V163A) that result in high expression levels of GFPuv in *Escherichia coli*, a more complete formation of the fluorophore and improved quantum yields of the fluorophore [21,22].

To answer the question of whether GFP, like DsbA, exhibits almost unlimited tolerance towards new termini in loop regions, we constructed 16 GFPuv variants with termini in different loops. As GFP consists of a continuous β-sheet as the central regular secondary structure, we also introduced new termini into four of the 11 β-strands of the β-barrel to examine whether new termini in this structural framework are tolerated to the same extent as the disruption of regular secondary structures in DsbA.

2. Materials and methods

2.1. Materials

Oligonucleotides were purchased from Eurogentec (Seraing, Belgium). DE52-cellulose was obtained from Whatman (Maidstone, UK) and phenyl sepharose and the Superdex 75 column were purchased from Amersham-Pharmacia (Buckinghamshire, UK). DNA-modifying enzymes and isopropyl-β,D-thiogalactoside (IPTG) were from AGS GmbH (Heidelberg, Germany) and Tfl-polymerase was from Promega (Madison, WI, USA). Phenylmethylsulfonyl fluoride

*Corresponding author. Fax: +41 (1) 633-1036.
E-mail: rudi@mol.biol.ethz.ch

[1] Present address: Department of Molecular and Cellular Biology, Harvard University, 7 Divinity Avenue, Cambridge, MA 02138, USA.

PII: S0014-5793(99)01044-3

(PMSF) and DNaseI were from Sigma (Deisenhofen, Germany) and lysozyme was obtained from Boehringer (Mannheim, Germany). Polyclonal rabbit anti-GFP antibodies were from Molecular Probes (Leiden, The Netherlands). The plasmid pGFPuv was purchased from Clontech (Palo Alto, CA, USA). All other chemicals were from Merck and of highest purity available (Darmstadt, Germany).

2.2. Plasmid construction

Codons for the Gly-Ser-$(Gly)_2$-Thr-Gly linker were appended to the ends of the mature *gfpuv* gene by the polymerase chain reaction (PCR), using the plasmid pGFPuv (Clontech) as template and the following oligonucleotide primers: N-terminal primer: 5′-CGA CGC GAA TTC TCT AGA TAA CGA GGG CAA CAT ATG GGT ACC GGT AGT AAA GGA GAA GAA CTT TTC (*Xba*I and *Kpn*I sites underlined); C-terminal primer: 5′-CGT GCG AGG CCT AGA TCT TAG GTA CCG CCG GAA CCT TTG TAG AGC TCA TCC ATG C (*Bgl*II and *Kpn*I sites underlined). The amplified gene was cloned into the plasmid pRBI-PDI [23] (accession code A22413) via the *Xba*I and *Bam*HI/*Bgl*I restriction sites. The *lac* repressor gene in the resulting plasmid was subsequently inactivated by deletion of a 522 bp fragment through digestion with *Pvu*II and *Bst*EII, treatment with T4 DNA polymerase and religation with T4 DNA ligase. The resulting plasmid (pGFPuv3) allowed strong expression of the *gfpuv* gene under control of the *lac* promotor/operator in the absence of IPTG.

For construction of circularly permuted *gfpuv* genes, a 729 bp fragment encoding residues 1–238 of GFPuv and the hexapeptide linker was generated by digestion of pGFPuv3 with *Kpn*I. The fragment was circularized by ligation with T4 DNA ligase. The circular gene with a continuous reading frame was isolated and used as PCR template for the amplification of the 20 circularly permuted *gfpuv* genes with 20 specific pairs of oligonucleotide primers. All amplified genes were cloned into the pGFPuv3 vector background and verified by dideoxynucleotide sequencing of the permuted *gfpuv* genes.

2.3. Expression levels of circularly permuted GFPuv variants

Cells of *E. coli* JM83 [24] harboring the expression plasmids for wild-type GFPuv or the 20 circularly permuted variants were grown at 25°C in 2×YT medium containing 100 μg/ml ampicillin. After induction with 1.0 mM IPTG at an optical density at 550 nm (OD_{550}) of 1.0, the cells were further grown for 16 h and harvested. After suspension in 1/100 vol. of PBS buffer (20 mM sodium phosphate, 115 mM NaCl pH 7.4) the cells were lysed by sonication, and samples from the soluble and insoluble fractions of the cell extracts (corresponding to an identical number of cells) were subjected to SDS-PAGE and immunoblotting. GFP-specific immunostaining was performed with polyclonal rabbit anti-GFP antibodies as described [4].

2.4. Purification of circularly permuted GFPuv variants

Cell growth in 1.5 l of 2×YT/amp medium and induction with IPTG was performed as described above. The cells were harvested, washed with 20 mM Tris/HCl pH 8.0, resuspended in the same buffer containing lysozyme and DNaseI (1 mg/ml and 10 μg/ml, respectively), incubated at 37°C for 30 min and disrupted by sonification (6×60 s, 0°C). After centrifugation, the supernatant was incubated at 50°C for 30 min and precipitated material was removed by centrifugation. The supernatant was mixed with PMSF (final concentration: 1.0 mM) and applied to a DE52 anion exchange column equilibrated with 20 mM Tris/HCl pH 8.0. GFPs were eluted with 0.5 M NaCl in 20 mM Tris/HCl pH 8.0 and the elute was mixed with 4.0 M ammonium sulfate to a final concentration of 0.8 M ammonium sulfate. The solution was applied to a phenyl sepharose column equilibrated with 20 mM Tris/HCl pH 8.0, 0.8 M ammonium sulfate, GFPs were eluted with 20 mM Tris/HCl pH 8.0 and dialyzed against PBS buffer. The solutions were concentrated to approximately 5 ml and applied to a HiLoad 26/60 Superdex 75 gel filtration column equilibrated with PBS. Fluorescent fractions were combined, dialyzed against 20 mM Tris/HCl pH 8.0 and, after adding 4.0 M ammonium sulfate to a final concentration of 0.8 M ammonium sulfate, rechromatographed on phenyl sepharose, using a linear gradient from 0.8 M to 0 M ammonium sulfate. Fluorescent fractions were pooled and dialyzed against distilled water. Typically, 90 mg of GFPuv wild-type were obtained with this procedure. The yields for the permuted variants varied between 10 and 90 mg.

2.5. Determination of extinction coefficients

Molar extinction coefficients for circularly permuted GFPuv variants were determined using the 'base-denatured chromophore' method [25,26]. Briefly, the absorbance spectra of the GFP variants were recorded at 25°C in PBS at protein concentrations of 1.0 μM. Samples were then diluted 1:1 with 0.2 M NaOH, incubated for 3 min and the absorbance spectra were recorded again and corrected for the volume increase. Molar extinction coefficients of the native variants at 397 and 475 nm in PBS were calculated using the known extinction coefficient for the base-denatured chromophore at 447 nm ($\varepsilon_{447\,nm} = 44\,000\ M^{-1}\ cm^{-1}$) [26]. Absorbance spectra were recorded on a Cary 3E absorbance spectrometer which guaranteed highest signal to noise ratio at low absorbance values. The estimated error of the measured molar extinction coefficients is below 2%.

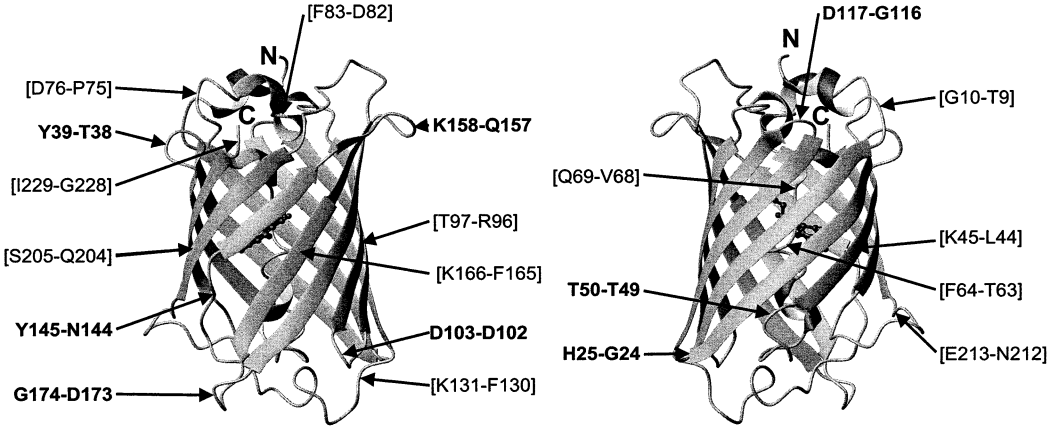

Fig. 1. Ribbon representations of the 3-dimensional structure of GFP [8] showing the positions of the newly introduced termini in the 20 circularly permuted GFPuv variants investigated in this study. Circularly permuted variants that were soluble in the *E. coli* cytoplasm and formed the intact chromophore are indicated in bold face. Variants that did not form the chromophore, accumulated in inclusion bodies or were degraded in the cytoplasm are given in brackets. The first and last resolved residues in the X-ray structure of GFP, S2 and I229, are indicated at the top of the 11-stranded β-barrel by (N) and (C), respectively. The GFP termini (residues 1 and 238) were connected by the hexapeptide linker Gly-Ser-$(Gly)_2$-Thr-Gly in all circularly permuted variants. The structure on the right is rotated by 180° about a vertical axis relative to the structure on the left. The nomenclature of the circularly permuted variants indicates the first and the last residue of the polypeptide chain (amino acid numbering according to wild-type GFP [13]). The chromophore formed by residues 65–67 in the center of the barrel is depicted in a ball-and-stick representation. The figure was generated with the program MOLMOL [38].

Table 1
Folding of circularly permuted GFPuv variants in the *E. coli* cytoplasm and physical properties of purified GFPuv variants

GFPuv variant	Position of new termini[a]	GFP fluorescence in the soluble fraction of the cell extract (+IPTG)	GFP level in the soluble fraction of the cell extract[b]	GFP level in the insoluble fraction of the cell extract[b]	$\varepsilon^{c}_{397\ nm}$ ($M^{-1}\ cm^{-1}$)	$\varepsilon^{c}_{475\ nm}$ ($M^{-1}\ cm^{-1}$)	Quantum yield[c] (λ_{ex} = 397 nm) (%)	Apparent T_m^c (°C)
w.t.	–	++++	++++	++++	30 500	14 150	79	81.9 ± 0.5
G10-T9	loop α1-β1	−	−	−				
H25-G24	loop β1-β2	+	+	+				
Y39-T38	loop β2-β3	+	++	++				
K45-L44	β3	−	+	++				
T50-T49	loop β3-α2	++	++	++	30 200	14 800	76	83.3 ± 0.5
F64-T63	loop α2-α3	−	+	++				
Q69-V68	loop α2-α3	−	−	−				
D76-P75	loop α3-α4	−	−	+				
F83-D82	loop α3-α4	−	−	+				
T97-R96	β4	−	+	++				
D103-D102	loop β4-β5	+	++	+++				
D117-G116	loop β5-β6	+	+	+				
K131-F130	loop β6-β7	−	+++	++++				
Y145-N144	loop β6-β7	++++	++++	++++	37 300	2300–2700	47	68.3 ± 0.5
K158-Q157	loop β7-β8	+++	+++	+++	30 500	14 100	74	> 75[d]
K166-F165	β8	−	+++	++++				
G174-D173	loop β8-β9	+++	+++	+++	31 500	14 000	70	79.5 ± 1.0
S205-Q204	β10	−	++	+				
E213-N212	loop β10-β11	−	+	+				
I229-G228	C-terminal tail	++++	++++	++++	30 000	14 000	76	79.1 ± 0.5

[a]Regular secondary structures are numbered according to [8]. The term 'loop' designates turns and elements of irregular secondary structure.
[b]The GFP level was detected by immunoblotting with rabbit anti-GFP antibodies. The levels of wild-type GFPuv in the soluble and insoluble fraction of the cell extract were set to (++++). However, note that only 10% of the total GFPuv protein is found in the insoluble fraction and 90% in the soluble fraction.
[c]Determined at pH 7.4 and protein concentrations where wild-type GFPuv is supposed to be essentially monomeric. The errors in molar extinction coefficients and quantum yields are below 2%.
[d]T_m could not be determined accurately due to irreversible aggregation.

2.6. Quantum yield measurements

Quantum yield measurements were performed at 25°C in PBS buffer and protein concentrations adjusted to an absorbance at 397 nm of 0.050. Fluorescence emission spectra between 450 and 650 nm (excitation at 397 nm) were integrated and compared with the fluorescence intensity of wild-type GFPuv, for which a quantum yield of 79% has been reported [22].

2.7. Thermal unfolding of GFPuv variants

GFPuv and circularly permuted variants were adjusted to an $A_{404\,nm} = 0.10$ in PBS buffer. Samples were heated from 30 to 95°C at a constant rate of 1°C min^{-1} in a stirred 1 ml quartz cuvette and the absorbance decrease at 404 nm was recorded. The data were normalized by correcting for the pre- and posttransitional baselines.

3. Results

3.1. Construction of circularly permuted variants of GFPuv

In the 1.9 Å X-ray structure of wild-type GFP from *A. victoria* the N-terminal residue and the C-terminal segment 230–238 are not resolved [8]. Although the C-terminal segment 230–238 is principally of sufficient length to span the distance between the first and last resolved residue (19 Å between the C^{α} atoms of S2 and I229) [8], we decided to introduce a hexapeptide linker (Gly-Ser-$(Gly)_2$-Thr-Gly) between the termini of GFPuv to account for the possibility that direct linkage of the natural termini leads to loss of folding competence of circularly permuted GFPuv variants. Fig. 1 shows the positions of the new termini in the 20 circularly permuted variants that were constructed and investigated in this study. In four of the constructs, new termini were introduced into strands of the central β-barrel, 14 constructs were made with termini within loops at the top and bottom of the β-barrel, and two of the variants, F64-T65 and Q69-V68, had new termini directly next to the chromophore segment S65-G67.

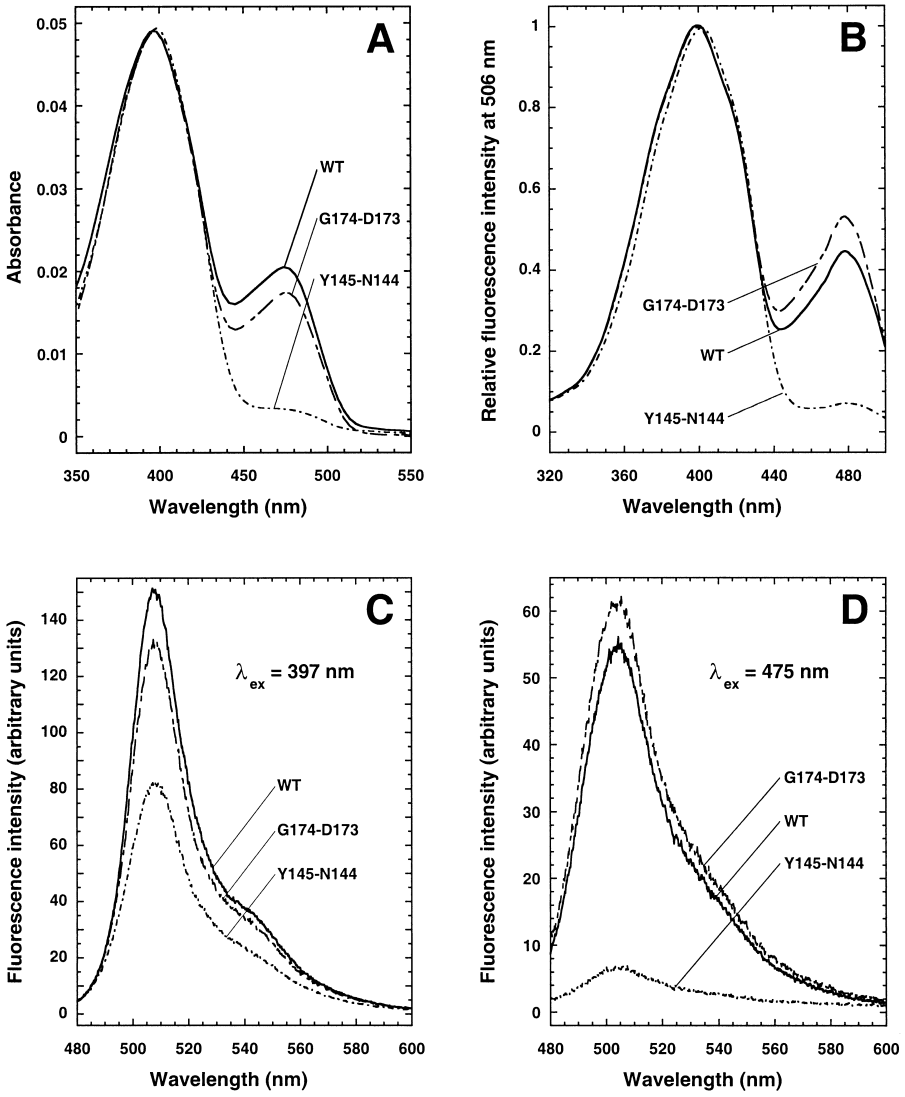

Fig. 2. Comparison of the spectroscopic properties of the chromophore in the circularly permuted GFPuv variants with the chromophore in wild-type GFPuv at pH 7.4 and 25°C. The permuted variants G174-D173 and Y145-N144, which showed the strongest spectral differences compared to the wild-type (cf. Table 1), are shown as examples. A: Absorbance spectra. For best comparison, the protein concentrations (1.4–1.7 μM) were adjusted such that the absorbance at 397 nm (first absorbance maximum) was identical in all samples. B: Fluorescence excitation spectra recorded at an emission wavelength of 506 nm (same samples as in A). C and D: Fluorescence emission spectra at identical protein concentrations (1.0 μM). Proteins were excited either at 397 nm (first absorbance maximum) (C) or at 475 nm (second absorbance maximum) (D).

3.2. Folding of the circularly permuted GFPuv variants in vivo

We first expressed wild-type GFPuv and its 20 circularly permuted variants at 25°C in *E. coli*. Folding of the GFP variants in vivo was analyzed by immunostaining after separation of the soluble and insoluble fractions of the cell extracts with SDS-PAGE, and by detection of the GFP-specific fluorescence at 506 nm in the soluble fractions (Table 1). Nine of the 20 permuted variants gave detectable GFP fluorescence in the soluble fraction of the cell extract, indicating that these variants fold and are capable of forming the chromophore. As expected, all fluorescent variants were detected in the soluble fraction, with a good correlation between protein concentration and fluorescence intensity in the extracts (Table 1). The fluorescent variants exclusively contained new termini in loop regions, whereas none of the four permuted proteins with termini in strands of the β-barrel showed chromophore formation.

Wild-type GFPuv and the permuted variants were also found in the insoluble fraction of the cell extract. In the case of wild-type GFPuv approximately 10% of the expressed protein accumulated in inclusion bodies. Only the variants G10-T9 and Q69-V68 could neither be detected in the soluble nor in the insoluble fraction (Table 1). Importantly, seven out of the 11 variants which were not capable of forming the chromophore in vivo were nevertheless detectable as soluble proteins in the cell extracts, with the loop variant K131-F130 and the β-strand variant K166-F165 almost reaching wild-type levels in the soluble fractions (Table 1).

3.3. Spectroscopic properties of the circularly permuted variants

For further characterization of the fluorescent circularly permuted variants, the mutant proteins with the highest expression levels were purified, i.e. T50-T49, Y145-N144, K158-Q157, G174-D173 and I229-G228. As wild-type GFPuv has been reported to form homodimers with a dissociation constant of 20–100 μM [27,28], we compared the spectroscopic properties of the purified fluorescent variants with those of wild-type GFPuv at identical protein concentrations of 1.0 μM where GFPuv is supposed to be essentially monomeric.

Like wild-type GFPuv, the permuted variants exhibit two absorbance maxima at 397 and 475 nm which are characteristic for the protonated and deprotonated form of the chromophore, respectively [29–31]. The only exception is the variant Y145-N144 which almost completely lacks the second absorbance maximum at 475 nm (Fig. 2A) and shows an increased extinction coefficient at 397 nm (Table 1). In all other purified variants, the absolute values of the extinction coefficients at 397 and 475 nm are very similar to the values measured for wild-type GFPuv. The same holds true for the ratios between the extinction coefficients at 397 and 475 nm indicating that the environment of the chromophore in the variants T50-T49, K158-Q157, G174-D173 and I229-G228 should be very similar to that in wild-type GFPuv.

Similar observations were made for the fluorescence properties of the purified permuted proteins. Like GFPuv wild-type, all variants show an emission maximum of 506 nm with quantum yields of 70–76% (excitation at 397 nm), which compares with a quantum yield of 79% in the wild-type [22] (Fig. 2B, C, Table 1). Again, the variant Y145-N144 is the only exception as it shows a significantly lower quantum yield of 47%. In addition, as expected from the almost complete lack of the second absorbance maximum, it shows practically no fluorescence when excited at 475 nm (Fig. 2B–D).

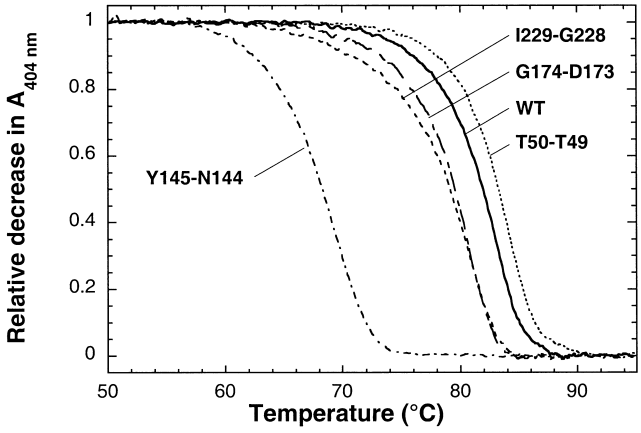

Fig. 3. Normalized thermal unfolding transitions of the purified circularly permuted GFPuv variants at pH 7.4 and protein concentrations of 2.8–3.5 μM, monitored by the decrease in chromophore absorbance at 404 nm. The heating rate was 1°C min^{-1}.

3.4. Stability of the circularly permuted variants against thermal denaturation

In order to investigate differences in stability between GFPuv wild-type and the circularly permuted variants, we measured thermal unfolding transitions of the proteins at concentrations of 2.8–3.5 μM, pH 7.4 and a constant heating rate of 1.0°C min^{-1}. The transitions were followed by the decrease in absorbance at 404 nm. This wavelength represents the maximum of the absorbance difference spectrum for the chromophore in native and heat-denatured GFPuv (heat-denatured GFPuv only shows a single absorbance peak at 383 nm; data not shown). GFPuv wild-type and the permuted variants T50-T49, G174-D173 and I229-G228 exhibit cooperative thermal unfolding transitions (Fig. 3) which proved to be up to 70% reversible when the heat-denatured proteins were incubated for less than 5 min at 95°C. Only the permuted variant K158-Q157 aggregated irreversibly during thermal unfolding. Surprisingly, the remarkable stability against thermal unfolding of GFPuv wild-type, which has an apparent melting temperature (T_m) of 81.9°C, was essentially retained in the permuted variants (Fig. 3, Table 1), and the thermal stability of the variant T50-T49 (T_m = 83.3°C) even exceeds that of the wild-type. Again, the variant Y145-N144 showed the strongest differences to the wild-type and the other permuted proteins. It is the least stable variant with an apparent T_m of 68.3°C, but is still a very stable protein (Fig. 3, Table 1).

4. Discussion

All circularly permuted variants of GFPuv investigated in this study were designed such that the new termini were introduced at solvent accessible positions on the surface of the GFP structure. Although the introduction of new termini into loop regions generally does not lead to a loss of folding competence of circularly permuted proteins [4], only nine out of the 16 GFPuv variants with termini in loops were capable of forming the chromophore. Moreover, none of the four GFPuv variants with termini in β-strands adopts a conformation with intact chromophore. The relatively low fraction of

folding-competent GFPuv variants may be explained by strong cooperative interactions stabilizing the 11-stranded β-barrel of GFP, and by relatively strong contributions of the loop regions to the overall stability of GFP.

The folding pathway of GFP differs from folding of other one-domain proteins in that the covalent structure of the protein changes irreversibly during the folding process. The newly synthesized GFP polypeptide must first adopt a conformation that allows the spontaneous, intramolecular cyclization of segment 65–67, which is subsequently converted to the intact chromophore by air oxidation [32]. The folding reaction thus involves at least two intermediates, i.e. a folded form of the polypeptide prior to cyclization of residues 65–67, and a folded conformation with the reduced form of the chromophore [32]. This strict requirement for folding intermediates that may be as defined as the native protein with intact chromophore is in apparent contrast to the emerging view that multiple pathways coexist for productive folding to the thermodynamically most stable state [33]. The dependence of chromophore formation on well-defined intermediates would provide another explanation for the low tolerance of GFPuv towards new termini, as many of the new termini might abolish interactions that are required for formation and stability of these intermediates.

Like wild-type GFPuv, all fluorescent variants that were purified and characterized further exhibit high stability against thermal unfolding. The least stable variant Y145-N144 with a T_m of 68.3°C is still a very stable protein (Table 1, Fig. 3). The thermal stability of the permuted variant T50-T49 is even slightly higher than that of wild-type GFPuv. Although we cannot deduce thermodynamic parameters from the thermal unfolding transitions, this variant appears to be the first case of a circularly permuted protein that is more stable than the wild-type. In contrast, all other circularly permuted protein variants that have been described so far showed a lower stability than the natural protein [4]. A simple explanation for the high stability of the permuted GFPuv variants would be a strong contribution of the chromophore to GFP stability. A dominant role of the chromophore would guarantee high protein stability once the intact chromophore is formed. The environment of the chromophore in all purified permuted variants is indeed very similar to that in wild-type GFPuv, as evidenced by the spectroscopic properties of the chromophores. Only the variant Y145-N144 has significantly different absorbance spectra, with a loss of the absorbance peak at 475 nm. The spectroscopic differences may be due to the close proximity of residues N144 and Y145 to the GFP chromophore relative to the new termini in the other GFPuv variants with intact chromophore [8].

Terminal deletions in GFP have shown that residues 7–229 are still sufficient for GFP folding and chromophore formation [34]. While the presence of I229 was found to be essential for GFP folding, the transfer of I229 from the C-terminal segment to the N-terminus in the permuted variant I229-G228 had no influence on folding. The importance of loop regions for GFP stability is further illustrated by the fact that all reported deletions of residues within loop regions of GFP have resulted in loss of folding competence [34,35]. Two of these internal loop deletions coincide with the loop disruptions in the circularly permuted variants D76-P75 and F83-D82 which were not capable of forming the chromophore (Table 1).

Some loop regions of GFP have recently been used for the insertion of peptide segments and the construction of peptide libraries using GFP as a scaffold [36,37]. For example, peptide libraries can be inserted into the peptide bond 172–173 of loop β8-β9 without loss of folding competence [37], which agrees with the efficient folding of the permuted variant G174-D173 where the same loop is disrupted. However, two of our permuted variants yielded different results compared to the reported insertion experiments. While insertions into the peptide bond 49–50 strongly reduced the yields of fluorescent GFP, the permuted variant T50-T49 could efficiently fold in vivo. Conversely, the permuted variant D117-G116 was only obtained in very low yields, while insertions between the residues 116 and 117 had no significant effect on GFP folding efficiency [36].

In conclusion, the circularly permuted GFP variants investigated in this study show that GFP exhibits a lower tolerance towards circular permutations compared to other proteins. Our data support the view that cooperative interactions within the 11-stranded β-barrel are essential for GFP folding, and that the chromophore strongly contributes to GFP stability.

Acknowledgements: Discussions with Dr. B. Steipe and J. Wiehler are gratefully acknowledged. This project was supported by the ETH Zürich.

References

[1] Thornton, J.M. and Sibanda, B.L. (1983) J. Mol. Biol. 167, 443–460.
[2] Goldenberg, D.P. and Creighton, T.E. (1983) J. Mol. Biol. 165, 407–413.
[3] Luger, K., Hommel, U., Herold, M., Hofsteenge, J. and Kirschner, K. (1989) Science 243, 206–210.
[4] Hennecke, J., Sebbel, P. and Glockshuber, R. (1999) J. Mol. Biol. 286, 1197–1215.
[5] Graf, R. and Schachman, H.K. (1996) Proc. Natl. Acad. Sci. USA 93, 11591–11596.
[6] Ormo, M., Cubitt, A.B., Kallio, K., Gross, L.A., Tsien, R.Y. and Remington, S.J. (1996) Science 273, 1392–1395.
[7] Wu, C.-K., Liu, Z.-J., Rose, J.P., Inouye, S., Tsuji, F., Tsien, R.Y., Remington, S.J. and Wang, B.C. (1997) in: Bioluminescence and Chemiluminescence (Hastings, J., Kricka, L.J. and Stanley, P.E., Eds.), pp. 399–402, Wiley, Chichester.
[8] Yang, F., Moss, L.G. and Phillips Jr., G.N. (1996) Nat. Biotechnol. 14, 1246–1251.
[9] Cody, C.W., Prasher, D.C., Westler, W.M., Prendergast, F.G. and Ward, W.W. (1993) Biochemistry 32, 1212–1218.
[10] Cubitt, A.B., Heim, R., Adams, S.R., Boyd, A.E., Gross, L.A. and Tsien, R.Y. (1995) Trends Biochem. Sci. 20, 448–455.
[11] Niwa, H., Inouye, S., Hirano, T., Matsuno, T., Kojima, S., Kubota, M., Ohashi, M. and Tsuji, F.I. (1996) Proc. Natl. Acad. Sci. USA 93, 13617–13622.
[12] Heim, R., Prasher, D.C. and Tsien, R.Y. (1994) Proc. Natl. Acad. Sci. USA 91, 12501–12504.
[13] Prasher, D.C., Eckenrode, V.K., Ward, W.W., Prendergast, F.G. and Cormier, M.J. (1992) Gene 111, 229–233.
[14] Nishiuchi, Y., Inui, T., Nishio, H., Bodi, J., Kimura, T., Tsuji, F.I. and Sakakibara, S. (1998) Proc. Natl. Acad. Sci. USA 95, 13549–13554.
[15] Bokman, S.H. and Ward, W.W. (1981) Biochem. Biophys. Res. Commun. 101, 1372–1380.
[16] Ward, W.W. and Bokman, S.H. (1982) Biochemistry 21, 4535–4540.
[17] Kneen, M., Farinas, J., Li, Y. and Verkman, A.S. (1998) Biophys. J. 74, 1591–1599.
[18] Llopis, J., McCaffery, J.M., Miyawaki, A., Farquhar, M.G. and Tsien, R.Y. (1998) Proc. Natl. Acad. Sci. USA 95, 6803–6808.
[19] Miyawaki, A., Llopis, J., Heim, R., McCaffery, J.M., Adams, J.A., Ikura, M. and Tsien, R.Y. (1997) Nature 388, 882–887.

[20] Misteli, T. and Spector, D.L. (1997) Nat. Biotechnol. 15, 961–964.
[21] Crameri, A., Whitehorn, E.A., Tate, E. and Stemmer, W.P. (1996) Nat. Biotechnol. 14, 315–319.
[22] Patterson, G.H., Knobel, S.M., Sharif, W.D., Kain, S.R. and Piston, D.W. (1997) Biophys. J. 73, 2782–2790.
[23] Wunderlich, M. and Glockshuber, R. (1993) J. Biol. Chem. 268, 24547–24550.
[24] Yanisch-Perron, C., Vieira, J. and Messing, J. (1985) Gene 33, 103–119.
[25] Ward, W.W., Cody, C., Hart, R.C. and Cormier, M.J. (1980) Photochem. Photobiol. 31, 611–615.
[26] Ward, W.W. (1981) in: Bioluminescence and Chemiluminescence: Basic Chemistry and Analytical Applications (DeLuca, M. and McElroy, D.W., Eds.), pp. 235–242, Academic Press, New York.
[27] Phillips Jr., G.N. (1997) Curr. Opin. Struct. Biol. 7, 821–827.
[28] Clontech Laboratories (1997) Living Colors User Manual PT2040-1, p. 12.
[29] Chattoraj, M., King, B.A., Bublitz, G.U. and Boxer, S.G. (1996) Proc. Natl. Acad. Sci. USA 93, 8362–8367.
[30] Palm, G.J., Zdanov, A., Gaitanaris, G.A., Stauber, R., Pavlakis, G.N. and Wlodawer, A. (1997) Nat. Struct. Biol. 4, 361–365.
[31] Lossau, H., Kummer, A., Heinecke, R., Pollinger-Dammer, F., Kompa, C., Bieser, G., Jonsson, T., Silva, C.M., Yang, M.M., Youvan, D.C. and Michel-Beyerle, M.E. (1996) Chem. Phys. 213, 1–16.
[32] Reid, B.G. and Flynn, G.C. (1997) Biochemistry 36, 6786–6791.
[33] Baldwin, R.L. (1995) J. Biomol. NMR 5, 103–109.
[34] Li, X., Zhang, G., Ngo, N., Zhao, X., Kain, S.R. and Huang, C.C. (1997) J. Biol. Chem. 272, 28545–28549.
[35] Dopf, J. and Horiagon, T.M. (1996) Gene 173, 39–44.
[36] Abedi, M.R., Caponigro, G. and Kamb, A. (1998) Nucleic Acids Res. 26, 623–630.
[37] Doi, N. and Yanagawa, H. (1999) FEBS Lett. 453, 305–307.
[38] Koradi, R., Billeter, M. and Wüthrich, K. (1996) J. Mol. Graph. 14, 51–55.